View Online
Dynamic Article Links

Journal of
Materials Chemistry

Cite this: *J. Mater. Chem.*, 2011, **21**, 3178

www.rsc.org/materials

PAPER

Photoluminescent ZnO nanoparticles synthesized at the interface between air and triethylene glycol†

Huan-Ming Xiong,* Ri-Zhao Ma, Su-Feng Wang and Yong-Yao Xia

Received 7th August 2010, Accepted 6th December 2010
DOI: 10.1039/c0jm02577a

ZnO nanoparticles with bright photoluminescence and different colors were synthesized through a very facile sol–gel method in triethylene glycol solvent at room temperature. Unexpectedly, the solvent molecules were found to be oxidized by air in the presence of LiOH and finally modified on ZnO nanoparticles. The molar ratio between LiOH and zinc acetate controlled the morphology and optical properties of the products. When LiOH was in excess, the as-prepared ZnO nanoparticles had a negatively-charged surface, which exhibited highly stable and blue fluorescence due to electrostatic repulsion between the particles.

1. Introduction

ZnO nanomaterials, as kinds of cheap and non-toxic semiconductors, have shown great potential in the fields of UV lasers,[1] biomedical labels[2] and solar cells.[3] The synthetic methods leading to ZnO nanoparticles include traditional sol–gel routes,[4] hydrothermal–solvothermal syntheses,[5] organometallic synthetic methods[6] and novel sonochemical techniques.[7] Among them, the sol–gel routes are the most popular because they can expediently produce ZnO nanoparticles with visible fluorescence at rather low cost. ZnO nanoparticles resulting from sol–gel methods have controllable particle diameters of 1∼10 nm and plenty of defects on the surface. Thus, ZnO visible emission based on quantum size effects and electron–hole recombination at defects is realized through a simple sol–gel synthesis. In contrast, those ZnO nanocrystals prepared at high temperature,[5,6] although having better crystallinity and purity, exhibit weak fluorescence in the visible spectrum. Therefore, ZnO nanoparticles with a highly visible emission always have a high concentration of defects, which means that they are small, amorphous and protected well by proper ligands or shells.[8]

The traditional sol–gel route of preparing ZnO nanoparticles is hydrolysing zinc acetate in ethanol, which requires refluxing zinc acetate in absolute ethanol for 3 h, followed by reacting it with LiOH under sonication.[9] The as-prepared ZnO nanoparticles are not very stable because the small acetate groups cannot protect the ZnO sufficiently. As a result, the emission color of the obtained colloids turns rapidly from blue to green within a few minutes, and then slowly from green to yellow within several days.[10] In order to protect ZnO more sufficiently, we grafted polyethylene glycol methyl ether (PEGME) groups onto the ZnO surface by hydrolysing a new zinc salt having a large anion derived from PEGME.[11,12] The as-prepared PEGME-ZnO nanocomposites showed very stable luminescence, which could be adjusted from blue to yellow. However, this synthetic route required multi-step reactions and complex treatments that take much time.

Here, we show a very facile sol–gel route to synthesize ZnO nanoparticles protected by triethylene glycol (TEG) in one-pot at room temperature. TEG was chosen as the solvent, but finally the nanoparticles were modified on the ZnO nanoparticle surface through covalent bonds between the newborn carboxyl groups and Zn^{2+} ions. Infrared analyses disclose the TEG oxidation mechanism in the presence of LiOH and air. The evolution of the ZnO optical properties have been studied with respect to various molar ratios of [LiOH]/[Zn], and the results are quite different from those reported previously.

2. Experimental

$Zn(Ac)_2 \cdot 2H_2O$ and $LiOH \cdot H_2O$ were dissolved together in TEG at room temperature in beakers by stirring. The concentration of zinc was fixed at 0.1 M, while the molar ratio of [LiOH]/[Zn] was 1, 1.5 and 2, respectively. The solutions were exposed to the air and stirred for 1 month. For UV-vis absorption and photoluminescence (PL) measurements, a small amount of solution was extracted from the reactants and diluted by absolute ethanol at different times. For thermal analyses and IR spectrum measurements, excess ethyl acetate was added into each TEG solution to precipitate the white ZnO gel. The gel was washed with ethyl acetate and centrifuged, followed by drying in a vacuum oven at 100 °C.

PL spectra were recorded by a Varian Cary Eclipse fluorescence spectrophotometer. The UV-vis absorption data were recorded by a Perkin-Elmer Lambda 40 UV-vis spectrometer.

Department of Chemistry and Shanghai Key Laboratory of Molecular Catalysis and Innovative Materials, Fudan University, Shanghai, 200433, P. R. China. E-mail: hmxiong@fudan.edu.cn

† Electronic supplementary information (ESI) available: See DOI: 10.1039/c0jm02577a

A rhodamine 6G ethanol solution (QY = 95%) was used as the standard when evaluating the quantum yield of the ZnO colloids. Transmission electron microscope (TEM) images were obtained using a JEM-2010 transmission electron microscope operating at 200 kV. Infrared measurements were conducted on a Nicolet Impact 360 FTIR spectrometer. Thermogravimetric (TG) analyses were carried out using a Perkin-Elmer TGA 7 thermal analyzer.

3. Results and discussion

The molar ratio of [LiOH]/[Zn] (designated as R) in sol–gel routes is usually adjusted to control the emission color and particle size of ZnO nanoparticles, but the mechanisms involved are very controversial.[11–15] In ethanol solutions, $R = 1.4$ was regarded as the isoelectric point of the ZnO nanoparticles.[9,15] At this point, the zinc acetate was hydrolyzed totally to produce acetate-modified ZnO nanoparticles, of which the surface charge was zero. When R was smaller than 1.4, zinc acetate could not be hydrolyzed sufficiently, and the products were ZnO nanoparticles adsorbed with Zn^{2+} ions. When R was larger than 1.4, excess OH^- could exchange the acetate groups on the ZnO surface, and thus more and more OH groups would be modified on the ZnO particle surface. When R was close to 2, the solution became turbid and the ZnO nanoparticles precipitated, indicating that ZnO nanoparticles grafted with too many OH groups were agglomerating heavily. It is interesting that adding more LiOH into the reaction solution could dissolve such ZnO precipitates. When R reached 3.5, the as-prepared ZnO colloids turned transparent and exhibited a strong blue fluorescence.[11–13] Such a phenomenon was interpreted as being excess LiOH depositing on the ZnO surface to form a protective shell,[13] and thus the ZnO nanoparticles were small enough to emit blue light. Recently, the pH value was suggested to be the key to controlling ZnO growth and ZnO emission color,[15] *i.e.*, at lower pH values (with less LiOH), ZnO nuclei form slowly so that the final ZnO nanoparticles are larger, while at higher pH values (with more LiOH), ZnO nuclei form faster so that the final ZnO nanoparticles are smaller. Moreover, the authors ascribe the red-shift of the ZnO emission to an increase in surface oxygen vacancies, because at lower pH values, there are more Zn^{2+} ions, *i.e.*, oxygen vacancies on the ZnO surface. However, this model could not explain why their ZnO nanoparticles precipitated at all pH values and why at higher pH values the ZnO samples exhibited a higher quantum yield, even though they had less oxygen vacancies.

In the present TEG solutions, the situation is quite different from those in ethanol. First, in a wide range of R values (0.1∼10), the obtained ZnO colloids are transparent and stable for at least 1 week. Secondly, when $R < 0.5$ the luminescence of ZnO colloids is rather weak, and when $R > 1.8$ the ZnO nanoparticles do not precipitate but exhibit a strong blue emission. Thirdly, when $R > 2$ the solution turns yellow gradually, indicating some unknown reactions. Hence, R was adjusted in the range 1.0∼2.0 for this work. After 3 days' reaction at room temperature, photos of the ZnO colloids under UV light in Fig. 1 clearly show that the ZnO emission color changes from yellow to blue when the R value increases from 1 to 2. The emission color change of semiconductor quantum dots such as CdSe and CdTe is usually ascribed to quantum size effects,[16] *i.e.*, below the Bohr radius, the

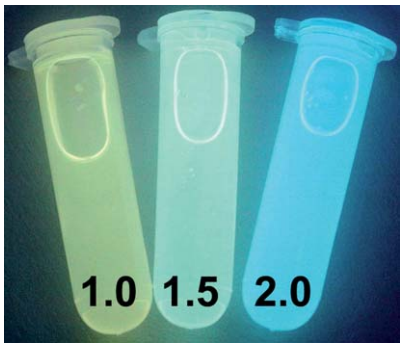

Fig. 1 TEG-ZnO colloids under UV light. The synthetic molar ratio of [LiOH]/[Zn] are 1.0, 1.5 and 2.0, respectively.

increase of nanoparticle size renders a decrease of their band gap and a red-shift of the corresponding exciton emission. However, the visible emission of ZnO quantum dots is not exciton emission. The ZnO band gap is 3.4 eV at room temperature, so ZnO exciton emission is located in the ultraviolet region. The mechanisms for ZnO visible emission are still controversial. Most recently, Yin *et al.*[17] suggested that ZnO visible emission is due to the transition of holes from the valence band to a pre-existing energy level, which is inconsistent with the widely accepted van Dijken model[18] where ZnO visible emission originates from the transition of an electron from the conduction band to a deep trap. Nevertheless, most scientists believe that ZnO visible emission arises from its defects, especially oxygen vacancies.[17–23] Since the energy levels of defects depend on both the band gap (determined by ZnO particle size) and the ZnO surface state, those factors that influence the ZnO surface state are also able to control the ZnO emission color. These factors include defects on the ZnO surface, the aggregation of ZnO nanoparticles, organic ligands and inorganic shells around ZnO particles, and the adsorption of solvents and ions. In fact, the TEM images (Fig. 2)

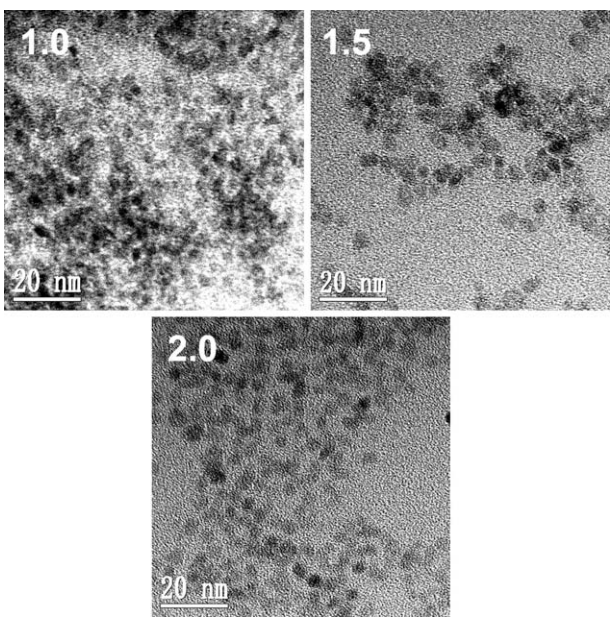

Fig. 2 TEM images of TEG-ZnO prepared using different [LiOH]/[Zn] ratios.

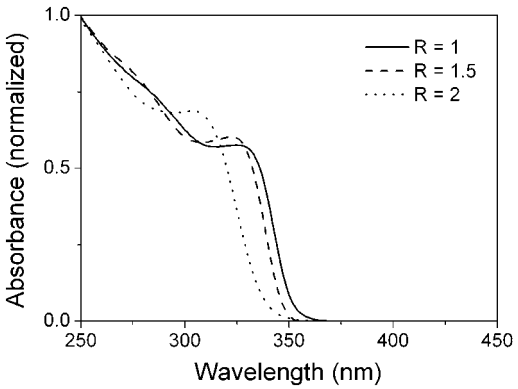

Fig. 3 UV-vis absorption spectra of TEG-ZnO ethanol solutions.

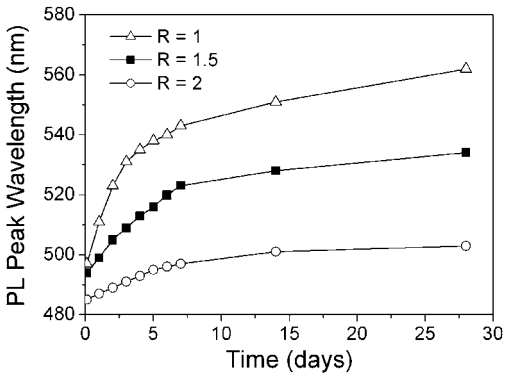

Fig. 5 The wavelengths for PL emission maxima of TEG-ZnO ethanol solutions at different times.

illustrate that the three ZnO samples have similar particle sizes (about 3∼4 nm) but their dispersion degrees differ significantly. The ZnO ($R = 2$) particles are uniform and monodisperse, while ZnO ($R = 1$) particles aggregate heavily. Hence, the red-shift of the emission color of these samples is mainly due to a surface state change induced by agglomeration.[9] When nanoparticles agglomerate tightly, the electron clouds of different particles will overlap with each other and electron tunneling will take place. As a result, the gaps between the energy levels will reduce so as to render the PL emission red-shifted. To study the luminescence mechanism of our ZnO nanoparticles, we measured the fluorescence decay curves and electron paramagnetic resonance (EPR) data of these samples (see the ESI†). The results show that ZnO visible emission mainly arises from the surface defects, in accordance with the following spectral shift.

The UV-vis absorption (Fig. 3) and PL (Fig. 4) spectra of the above three samples are in accordance with Fig. 1 and Fig. 2. Both the UV-vis absorption onsets and the PL excitation/emission peaks red-shift as the ZnO nanoparticles aggregate. These data represent the typical performance of ZnO nanoparticles, *i.e.*, the absorption onset and excitation maximum increasing from 320 to 340 nm corresponds to the emission peak red-shifting from 480 to 540 nm. Actually, for every sample, both the UV-vis absorption curves and the PL excitation/emission bands were red-shifting slowly and continuously from the start of the reaction. The peak positions of the PL emission and quantum yield for each ZnO sample were recorded at different times in Fig. 5 from the 3rd hour to the 28th day after dissolving the reactants in TEG. The emission peaks of all three samples red-shifted rapidly within the first week but the shift rate slowed down later, indicating that the ZnO nanoparticles grew mainly during the first week. In the subsequent three weeks, the reactants and products reached equilibrium and Ostwald ripening made the emission wavelength red-shift continuously. During the whole observation period, the particle growth rate followed the order ZnO ($R = 1$) > ZnO ($R = 1.5$) > ZnO ($R = 2$), which is in accordance with the QY evolution in Fig. 6.

The QY of ZnO colloids are influenced by the concentration of defects, the aggregation of nanoparticles and those species adsorbed on the ZnO surface, including ligands, ions and solvents. In a prototypical ZnO nanoparticle, defects are located mainly on its surface, and thus the smaller the particle size the higher the QY it exhibits.[24] After the initial nucleation, ZnO nanoparticles grow and consume the nutrients from the mother solution. In the meantime, some nanoparticles aggregate due to insufficient protection. Further growth will decrease the defect concentration, and nanoparticle aggregation will cause self-absorption and concentration effects.[25] As a result, the QY of ZnO colloids usually increases fast until the nucleation is complete and numerous ZnO nanoparticles have formed, and then the QY of the ZnO colloids decreases slowly due to further nanoparticle growth, crystallization and aggregation. Except for growth and aggregation, those species that are adsorbed onto ZnO surface are also important to ZnO luminescence. For

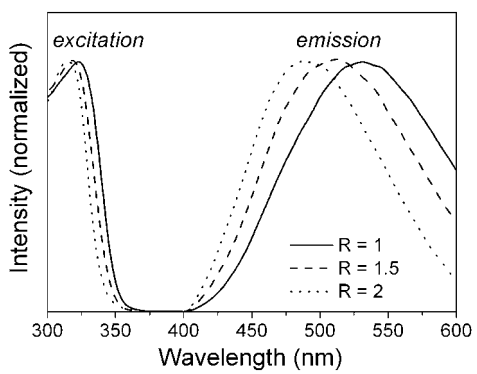

Fig. 4 PL excitation and emission spectra of TEG-ZnO ethanol solutions.

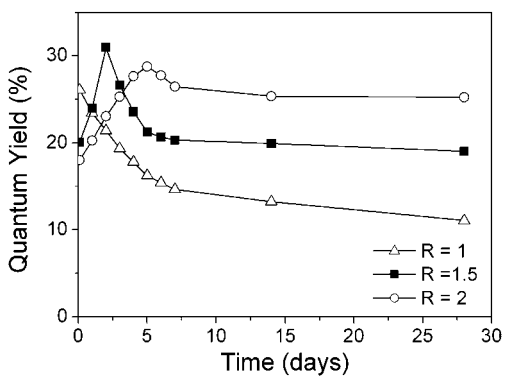

Fig. 6 Quantum yield of TEG-ZnO ethanol solutions at different times.

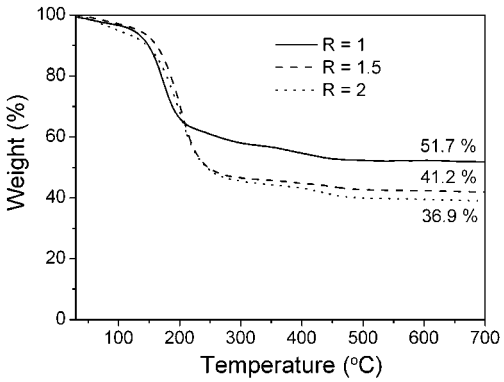

Fig. 7 TG curves of TEG-ZnO prepared by different [LiOH]/[Zn] ratios.

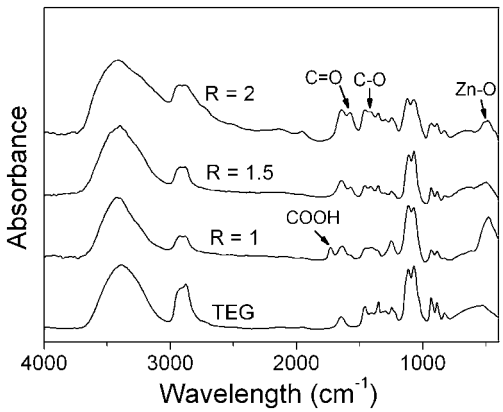

Fig. 8 IR spectra for TEG and ZnO nanoparticles prepared with different [LiOH]/[Zn] ratios.

example, many amines[26] and transition metal ions[27] are able to quench ZnO visible emission because they trap the photo-generated electrons or holes. Another fact is that excess Zn^{2+} ions can be adsorbed onto the ZnO surface[28] so that the oxygen vacancies on ZnO ($R = 1$) are more than those on ZnO ($R = 1.5$) and on ZnO ($R = 2$), and thus the QY of ZnO colloids follows the order ZnO ($R = 1$) > ZnO ($R = 1.5$) > ZnO ($R = 2$) at the early stage of particle growth (Fig. 6). Since a higher LiOH concentration renders faster nucleation and more nuclei,[15] the particle growth rate before the solution nutrients are exhausted should be in the sequence ZnO ($R = 1$) > ZnO ($R = 1.5$) > ZnO ($R = 2$). As a result, ZnO ($R = 1$) reached its QY maximum within 3 h, ZnO ($R = 1.5$) took 2 days and ZnO ($R = 2$) took 5 days. However, after reaching their QY maxima, the three samples exhibited different QY profiles. The QY of ZnO ($R = 1$) decreased continuously, the QY of ZnO ($R = 1.5$) decreased for 3 days significantly and then became stable, and the QY of ZnO ($R = 2$) only decreased slightly before reaching stability. Furthermore, after 4 weeks of stirring in beakers, the QY of ZnO ($R = 1$) was only 11% and the colloids were turbid, while the QY of the clear ZnO ($R = 1.5$) and ZnO ($R = 2$) colloids were 19% and 25%, respectively. These phenomena are completely different from a conventional ZnO QD performance in ethanol, indicating that TEG plays a key role in the reaction.

Thermal analyses and infrared measurements were employed to determine the composition of the three ZnO samples. Fig. 7 shows that the organic component in the ZnO nanoparticles increases as R increases. Although the three samples have similar particle sizes, their aggregation degrees are different. The ZnO ($R = 2$) particles are uniform and monodispersed, as shown in the TEM images, so it has the largest surface area to adsorb organic species. In general, organic species adsorbed onto ZnO surfaces can be easily washed away by the non-solvent,[10–12] but the TG data show that ZnO ($R = 1.5$) and ZnO ($R = 2$) possess over 50 wt% of organic components, which is far more than acetate could present.[25] If the excess organic components are chemically adsorbed TEG molecules, the result would be contrary to our previous report[7] that TEG does not adsorb onto a ZnO surface after a very similar reaction in an enclosed container. Therefore, not only TEG but also the air is involved in the present reaction. To verify this speculation, we performed a series of control experiments under a nitrogen atmosphere. The IR spectra of the air-free samples exhibited almost no TEG absorption (Fig. S2†), which proves that air is indispensable for modifying TEG on a ZnO surface.

IR analyses disclose the mechanism that ZnO ($R = 1$) nanoparticles aggregate heavily while ZnO ($R = 2$) nanoparticles are monodispersed. The IR spectra of these ZnO samples and the original TEG are compared in Fig. 8. The typical C–H vibration bands at 2900, 1460, 1350, 1250, 930 and 890 cm^{-1} are seen in all the ZnO samples, and the C–O–(H) vibration at 1072 cm^{-1} and the C–O–(C) vibration at 1112 cm^{-1} also prove that the TEG molecules have been modified on the ZnO surface. In comparison to TEG, the IR spectrum of ZnO ($R = 1$) shows a significant peak at 1730 cm^{-1} that is the typical of the C=O absorption of the COOH group,[11,12] indicating that the CH_2OH group on TEG has been oxidized by the air. This absorption at 1730 cm^{-1} is not observed in either ZnO ($R = 1.5$) or ZnO ($R = 2$) because at higher pH, COOH will be transformed into COO^- groups and coordinate with metal ions. We have reported that when Zn^{2+} ions are coordinated with COO^- groups in a unidentate form,[29] IR spectra will show a typical C=O vibration at 1580 cm^{-1} and a C–O vibration at 1425 cm^{-1}. In Fig. 8, all the ZnO samples show such two vibrations and a corresponding intensity increase as R increases, confirming that LiOH renders COOH to transform into COO^-. In the case of ZnO ($R = 2$) with excess LiOH, the TEG molecules on the ZnO surface have transformed into $^-OOCCH_2OCH_2CH_2OCH_2COO^-$ and thus the nanoparticles are negatively-charged. ZnO ($R = 2$) nanoparticles are monodispersed and very stable because of the electrostatic repulsion between them.[30] On the contrary, when $R = 1$ TEG is oxidized to $HOOCCH_2OCH_2CH_2OCH_2COOH$, which probably crosslinks the ZnO nanoparticles by the OH groups through hydrogen bonds or ester bonds. Therefore, ZnO ($R = 1$) nanoparticles aggregate heavily and the Zn–O band at 480 cm^{-1} is strong, while for well-dispersed ZnO ($R = 1.5$) and ZnO ($R = 2$), the corresponding Zn–O vibrations are rather weak.

4. Conclusion

Luminescent ZnO QDs were prepared through a very facile sol–gel method at room temperature. Their emission color was adjusted from blue to yellow and their quantum yields were in the range 10∼30%. Their optical properties were studied in detail

with respect to the [LiOH]/[Zn] molar ratio, R. IR analyses proved that in the presence of LiOH and air, TEG was oxidized to the dicarboxylic acid. With less LiOH ($R = 1$), such a dicarboxylic acid could crosslink ZnO nanoparticles and cause ZnO aggregation and precipitation. With more LiOH ($R = 2$), such a dicarboxylic acid transformed into anions and protected the ZnO nanoparticles effectively. These ZnO QDs with carboxyl groups can be grafted with biotins or antibodies so as to offer biomedical applications, and surface-charged ZnO nanoparticles are useful in self-assembly research.

Acknowledgements

This work was supported by the National Science Foundation of China Research project (grant no. 20873029) and the Shanghai Committee of Science and Technology (grant no. 09QA1400400).

References

1 A. B. Djurišić and Y. H. Leung, *Small*, 2006, **2**, 944.
2 H. M. Xiong, Y. Xu, Q. G. Ren and Y. Y. Xia, *J. Am. Chem. Soc.*, 2008, **130**, 7522.
3 A. E. Suliman, Y. W. Tang and L. Xu, *Sol. Energy Mater. Sol. Cells*, 2007, **91**, 1658.
4 L. Spanhel, *J. Sol-Gel Sci. Technol.*, 2006, **39**, 7.
5 Y. Chen, M. Kim, G. Lian, M. B. Johnson and X. Peng, *J. Am. Chem. Soc.*, 2005, **127**, 13331.
6 M. L. Kahn, M. Monge, V. Colliere, F. Senocq, A. Maisonnat and B. Chaudret, *Adv. Funct. Mater.*, 2005, **15**, 458.
7 H. M. Xiong, D. G. Shchukin, H. Möhwald, Y. Xu and Y. Y. Xia, *Angew. Chem., Int. Ed.*, 2009, **48**, 2727.
8 H. M. Xiong, *J. Mater. Chem.*, 2010, **20**, 4251.
9 L. Spanhel and M. A. Anderson, *J. Am. Chem. Soc.*, 1991, **113**, 2826.
10 E. A. Meulenkamp, *J. Phys. Chem. B*, 1998, **102**, 5566.
11 H. M. Xiong, D. P. Liu, Y. Y. Xia and J. S. Chen, *Chem. Mater.*, 2005, **17**, 3062.
12 H. M. Xiong, Z. D. Wang, D. P. Liu, J. S. Chen, Y. G. Wang and Y. Y. Xia, *Adv. Funct. Mater.*, 2005, **15**, 1751.
13 M. Abdullah, I. W. Lenggoro, K. Okuyama and F. G. Shi, *J. Phys. Chem. B*, 2003, **107**, 1957.
14 A. Glaria, M. L. Kahn, T. Cardinal, F. Senocq, V. Jubera and B. Chaudret, *New J. Chem.*, 2009, **32**, 662.
15 X. Tang, E. S. G. Choo, L. Li, J. Ding and J. Xue, *Chem. Mater.*, 2010, **22**, 3383.
16 X. G. Peng, L. Manna, W. D. Yang, J. Wickham, E. Scher, A. Kadavanich and A. P. Alivisatos, *Nature*, 2000, **404**, 59.
17 L. Zhang, L. Yin, C. Wang, N. Lun, Y. Qi and D. Xiang, *J. Phys. Chem. C*, 2010, **114**, 9651.
18 A. van Dijken, E. A. Meulenkamp, D. Vanmaekelbergh and A. Meijerink, *J. Phys. Chem. B*, 2000, **104**, 1715.
19 K. Vanheusden, W. L. Warren, C. H. Seager, D. R. Tallant, J. A. Voigt and B. E. Gnade, *J. Appl. Phys.*, 1996, **79**, 7983.
20 L. Guo, S. Yang, C. Yang, P. Yu, J. Wang, W. Ge and G. K. L. Wong, *Appl. Phys. Lett.*, 2000, **76**, 2901.
21 N. E. Hsu, W. K. Hung and Y. F. Chen, *J. Appl. Phys.*, 2004, **96**, 4671.
22 A. B. Djurišić, Y. H. Leung, K. H. Tam, Y. F. Hsu, L. Ding, W. K. Ge, Y. C. Zhong, K. S. Wong, W. K. Chan, H. L. Tam, K. W. Cheah, W. M. Kwok and D. L. Phillip, *Nanotechnology*, 2007, **18**, 095702.
23 H. B. Zeng, G. T. Duan, Y. Li, S. K. Yang, X. X. Xu and W. P. Cai, *Adv. Funct. Mater.*, 2010, **20**, 561.
24 A. van Dijken, J. Makkinje and A. Meijerink, *J. Lumin.*, 2001, **92**, 323.
25 S. Sakohara, M. Ishida and M. A. Anderson, *J. Phys. Chem. B*, 1998, **102**, 10169.
26 M. Chang, X. L. Cao, H. Zeng and L. Zhang, *Chem. Phys. Lett.*, 2007, **446**, 370.
27 X. T. Zhang, Y. C. Liu, J. Y. Zhang, Y. M. Lu, D. Z. Shen, X. W. Fan and X. G. Kong, *J. Cryst. Growth*, 2003, **254**, 80.
28 S. Monticone, R. Tufeu and A. V. Kanaev, *J. Phys. Chem. B*, 1998, **102**, 2854.
29 H. M. Xiong, X. Zhao and J. S. Chen, *J. Phys. Chem. B*, 2001, **105**, 10169.
30 D. P. Liu, G. D. Li, Y. Su and J. S. Chen, *Angew. Chem., Int. Ed.*, 2006, **45**, 7370.

